# Long non-coding RNA XIST promotes osteoporosis through inhibiting bone marrow mesenchymal stem cell differentiation

XI CHEN[1*], LEI YANG[1*], DAWEI GE[2*], WEIWEI WANG[3], ZHAOWEI YIN[1], JUNWEI YAN[1], XIAOJIAN CAO[2], CHUNZHI JIANG[1], SHENGNAI ZHENG[1] and BIN LIANG[1]

[1]Department of Orthopedic Surgery, Nanjing First Hospital, Nanjing Medical University, Nanjing, Jiangsu 210006; Departments of [2]Orthopedics and [3]Obstetrics and Gynecology, The First Affiliated Hospital of Nanjing Medical University, Nanjing, Jiangsu 210029, P.R. China

Received June 21, 2018; Accepted November 1, 2018

DOI: 10.3892/etm.2018.7033

**Abstract.** The purpose of the present study was to identify the key long non-coding (lnc)RNAs in the occurrence and development of osteoporosis (OP) and to explore the associated molecular mechanism. First, the Gene Expression Omnibus (GEO) datasets, with key words 'osteoporosis' and 'HG-133A', were screened. RankProd R package was used to calculate the dysregulated lncRNAs in OP. Following this, bone marrow mesenchymal stem cells (BM-MSCs) harvested from 3-week-old Sprague Dawley rats were employed for detection of osteoblast differentiation. Following overexpression or interference with X-inactive specific transcript (XIST), osteogenesis-associated genes and proteins in BM-MSCs were detected using reverse transcription-quantitative polymerase chain reaction and western blot analysis. Alkaline phosphatase (ALP) and Alizarin Red S staining were also performed to measure the osteogenic ability of BM-MSCs. Results from the two datasets indicated that 6 lncRNAs were dysregulated in OP. Notably, XIST is key lncRNA in diverse diseases, and was subsequently selected for analysis. It was revealed that XIST was significantly upregulated in plasma and monocytes from patients with OP compared with the normal controls. Furthermore, results indicated that overexpression of XIST significantly inhibited osteoblast differentiation in BM-MSCs, as evidenced by the decreased expression of ALP, bone γ-carboxyglutamic acid-containing protein and runt related transcription factor 2, reduced ALP activity and a decreased number of calcium deposits. However, interference of XIST exhibited the opposite biological effects in BM-MSCs. Taken together, XIST was highly expressed in the serum and monocytes of patients with OP. In addition, the findings suggested that XIST could inhibit osteogenic differentiation of BM-MSCs.

*Correspondence to:* Dr Shengnai Zheng or Dr Bin Liang, Department of Orthopedic Surgery, Nanjing First Hospital, Nanjing Medical University, 68 Changle Road, Nanjing, Jiangsu 210006, P.R. China
E-mail: zsn3280@sina.com
E-mail: ib15366110173@163.com

*Contributed equally

*Key words:* long noncoding RNA, X-inactive specific transcript, bone marrow mesenchymal stem cells, osteogenic differentiation

## Introduction

Osteoporosis (OP) is the most common type of skeletal disease, regardless of sex (1). As a progressive skeletal disease, OP is characterized by low bone mass and damaged bone structure, which can result in rarefaction of bone and an increased risk of fracture (2). In patients with fractures caused by OP, hip fractures are commonly observed (1). Previous evidence indicated that OP-induced factures are typically associated with higher fatality rates and can limit the activity of the patient, thereby increasing medical burden in China (1). According to the latest global research, it has been reported that menopausal women have the highest risk of OP (1). As age increases, the incidence rate of hip fracture in women aged between 55 and 59 is 34%, which is almost 5-fold greater (6.6%) in those aged >85 (3). Bone metabolism relies on the regulation between the osteoblasts and osteoclasts. In patients with OP, osteoclasts, which originate from the mononuclear macrophages of bone marrow hematopoietic stem cells, can enhance the bone absorption (4). Thus, research on the mononuclear cells is of great significance in enhancing the understanding on the mechanism and improving the treatment of OP.

Long non-coding (lnc)RNAs have a transcriptional length of >200 nucleotides and can regulate gene expression on various levels, including epigenetic, transcriptional and post-transcriptional regulation, without encoding any proteins (5-12). LncRNAs have become an area of interest in research, and it has been revealed that lncRNAs not only exist in the blood of patients with tumors, but are stably present, according to some reports, in the plasma or serum of some human non-neoplastic diseases (6). Hence, specific lncRNAs have been widely used in the diagnosis and treatment of various diseases, and may have potential clinical application value (13,14). This value provides a new direction in studying the etiology, pathogenesis and prognosis of

associated diseases. In recent years, circulating lncRNAs have been identified to serve an important role in diseases, including cardiovascular disease (15), refractory asthma (16), acute kidney injury (13), diabetes mellitus, major depressive disorder (17) and Hashimoto's thyroiditis (18). Nevertheless, a few studies have focused on the effects of circulating lncRNAs in OP.

In bone tissues, the activity of osteoblasts and osteoclasts is precisely coordinated (9,19). During bone remodeling, osteoclasts uptake the bone and then recruit bone marrow mesenchymal stem cells (BM-MSCs) for subsequent differentiation and bone formation (19). Under certain conditions, BM-MSCs possess the potential to differentiate into different types of cells, including osteoblasts, chondrocytes, adipocytes, muscle cells and tendon cells (20), which can provide a cell source for bone growth and bone repair. Osteoblasts are the primary functional cells in bone formation (20). They are distributed on the surface of bone, which can produce the organic components of the extracellular matrix as well as regulate the synthesis, secretion and mineralization of bone matrix (19,20). Notably, osteoblasts can be identified using the following indexes: Alkaline phosphatase (ALP), bridge proteins, bone morphogenetic proteins, and osteocalcin and bone sialoproteins (19,20). Furthermore, osteoclasts are distributed in the bone resorption lacuna, and are responsible for bone resorption (19,20).

There is a large number of experimental evidence suggesting that BM-MSCs are associated with OP. The present study aimed to assess the biological function of key long non-coding (lnc)RNAs in the occurrence and development of osteoporosis, and to further investigate its underlying molecular mechanism.

## Materials and methods

*Data collection*. Data retrieval was performed with the Gene Expression Omnibus (GEO) database (https://www.ncbi.nlm.nih.gov/geo/index.cgi) using 'osteoporosis' and 'HG-133A' as key words. A total of 10 datasets were identified. Since detection with the probe in HG-133A could identify various lncRNAs, the HG-133A platform was selected as the alternative platform in the present study. In the present study, a total of three datasets, GSE56815, GSE7158 and GSE2208, were acquired, in which GSE2208 was eliminated as this did not include the original CEL files. In the GSE56815 dataset, there were 40 microarrays in monocytes of normal bone and 40 of OP, whereas in the GSE7158 dataset there were 14 of normal bone and 14 of OP. Inclusion and exclusion criteria of OP was based on a previous guideline (21). Serum and blood cells of 40 cases were collected (14 males, 26 females; age range, 43-72 years) from patients admitted to The First Affiliated Hospital of Nanjing Medical University (Nanjing, Jiangsu, China) between July 2017 and February 2018. Written informed consent was obtained from all the participants. One tube of venous blood of all patients enrolled was collected immediately with an anticoagulant-free red blood collection tube following admission. The present study was approved by the Ethical Committee of Nanjing Medical University and patient consent was obtained prior to enrollment. The tube was placed in the refrigerator at 4˚C for 30 min, centrifuged at 2,500 x g for 15 min at room temperature, and then the upper serum was collected and placed in refrigerator at 20˚C.

*RankProd analysis of differential lncRNAs*. To comprehensively analyze the differentially expressed genes in the two datasets, analysis was performed with RankProd R package (22). Firstly, datasets were merged in accordance of the Combat method with the Slicomerging R package to eliminate the difference between the two groups (23). Proportion of false positives (pfp) of differentially expressed genes were identified using 1,000 permutations, and the list of upregulated or downregulated probes was determined on the basis of pfp (pfp<0.01) and fold change (FC) value (FC>1, upregulated; FC<1, downregulated).

*Isolation, culture and differentiation of BM-MSCs*. Primary BM-MSCs were collected from 10 3-week-old female Sprague-Dawley rats (weight range, 50-60 g) and the bone marrow was flushed from the femur and tibia of rats using a 5-ml syringe. All rats were housed in a temperature controlled room (21±2˚C), under a 12 h light/dark cycle, with free access to water and food. BM-MSCs were cultured in Dulbecco's modified Eagle's medium (DMEM; Gibco; Thermo Fisher Scientific, Inc., Waltham, MA, USA) supplemented with 10% fetal bovine serum (FBS; Gibco; Thermo Fisher Scientific, Inc.), 1% L-glutamine (Gibco; Thermo Fisher Scientific, Inc.), 1% penicillin and 1% HEPES (Gibco; Thermo Fisher Scientific, Inc.) in an atmosphere containing 5% $CO_2$ at 37˚C. Medium was changed every 2 days to remove unattached cells. Following 5 days of incubation, the primary cells were trypsinized and passaged. Generation 3-5 of BM-MSCs were used in the present study. Notably, 10% FBS, 10 nmol/l dexamethasone (Sigma-Aldrich; Merck KGaA, Darmstadt, Germany), 10 mmol/l β-glycerophosphate (Sigma-Aldrich; Merck KGaA), 50 $\mu$g/ml ascorbic acid (Sigma-Aldrich; Merck KGaA), 1% L-glucose, 1% penicillin-streptomycin and 1% HEPES were added to a high-glucose DMEM (DMEM-HG; Gibco; Thermo Fisher Scientific, Inc.) in order to make up the osteogenic medium and induce osteogenic differentiation of MSCs.

*Cell surface markers of MSCs*. MSC surface markers of cells isolated from rats were detected using flow cytometry with the following antibodies: Fluorescein isothiocyanate (FITC) hamster anti-rat cluster of differentiation (CD)29 (1:100; cat. no. 564131), FITC mouse anti-rat CD44H (1:100; cat. no. 550974), FITC mouse anti-rat CD45 (1:100; cat. no. 561587), FITC mouse anti-rat CD90 (1:100; cat no. 554894). All antibodies were purchased from BD Biosciences (Franklin Lakes, NJ, USA) and were incubated at 20˚C for 1 h. FITC Goat anti-Mouse Immunoglobulin G (H+L) Cross-Adsorbed Secondary Antibodies was purchased from Thermo Fisher Scientific, Inc. (1:1,000; cat. no. 31541) and incubated at 20˚C for 30 min. Human TruStain FcX™ (BioLegend, Inc., San Diego, CA, USA; cat. no. 422301) was used for blocking at room temperature for 5 min. Flow cytometer (FACSCalibur; BD Bioscience) was used for analysis. Data were obtained and analyzed using CellQuest professional software (Version 3.3; Becton, Dickinson and Company; Franklin Lakes, NJ, USA). Generation three

BM-MSCs were suspended in PBS, incubated with 0.5 $\mu$g/ml of each antibody. Unstained MSCs served as controls.

*Reverse transcription-quantitative polymerase chain reaction (RT-qPCR)*. Total RNA was extracted from BM-MSCs using TRIzol reagent (Invitrogen; Thermo Fisher Scientific, Inc.) according to the manufacturer's instructions. Total RNA concentration was measured using a NanoDrop 2000 (Thermo Fisher Scientific, Inc.) and 1 $\mu$g of total RNA was reverse transcribed into cDNA using a reverse transcription kit (Takara Bio, Inc., Otsu, Japan). RT-qPCR was performed on an ABI7900 Fast Real-Time System (Applied Biosystems; Thermo Fisher Scientific, Inc.) using the SYBR Premix Ex Taq kit (Takara Bio, Inc.). The thermocycling conditions were as follows: pre-denaturation at 95˚C for 5 min, denaturation at 95˚C for 30 sec, annealing at 60˚C for 45 sec, extension at 72˚C for 3 min, with 35 cycles and extension at 72˚C for 5 min. PCR products were then stored at 4˚C. The primers utilized in PCR were as follows: XIST forward, 5'-AGG CTGGCTGGAATAAAGG-3' and reverse, 5'-TATGAAAAG GGAGGCGTGGT-3'; ALP forward, 5'-GGGACTGGTACT CGGACAAT-3' and reverse, 5'-GGCCTTCTCATCCAGTTC AT-3'; Bglap forward, 5'-CATGAGGACCCTCTCTCTGC-3' and reverse, 5'-TGGACATGAAGGCTTTGTCA-3'; Runx2 forward, 5'-GCACCCAGCCCATAATAGA-3' and reverse, 5'-TTGGAGCAAGGAGAACCC-3'; GAPDH forward, 5'-GGCACAGTCAAGGCTGAGAATG-3' and reverse, 5'-ATGGTGGTGAAGACGCCAGTA-3'. The $2^{-\Delta\Delta Cq}$ method was used. GAPDH was used as a standard control for data analysis (24).

*Western blot analysis*. The proteins were extracted from BM-BMSCs. Subsequently, the protein concentration was detected using the BCA method (Pierce; Thermo Fisher Scientific, Inc.) and adjusted using the radioimmunoprecipitation assay (Beyotime Institute of Biotechnology, Shanghai, China). A total of 30 $\mu$g protein were loaded per lane for electrophoresis. Following SDS-PAGE (5% concentrated gel and 10% separation gel) the sample was transferred to a polyvinylidene fluoride (PVDF) membrane (EMD Millipore, Billerica, MA, USA), which was then soaked in 5% skimmed milk at room temperature for 1 h. The PVDF membrane was subsequently cut and respectively incubated with the following antibodies at 4˚C overnight: Runx2 (1:500; cat. no. ab76956); rabbit polyclonal ALP (1:500; cat. no. ab83259) and rabbit polyclonal GAPDH (1:500; cat. no. ab37168; all, Abcam, Cambridge, UK) The following day, the bands were washed three times with PBS (for 10 min each time). Subsequently, the bands were incubated with the following secondary antibodies for 1 h at 20˚C: Horseradish peroxidase conjugated goat anti-rabbit Immunoglobulin G (1:2,000; cat. no. ab6721; Abcam). Samples were then washed three times with PBS (for 10 min each time). Lastly, ECL solution (Merck KGaA) was applied to bands in order to detect the protein expression levels. Protein bands were analyzed using Image J software (Version 1.38; National Institutes of Health, Bethesda, MD, USA). GAPDH served as the internal control.

*Cell transfection*. BM-MSCs were resuspended in antibiotic-free DMEM and re-seeded into 6-well plates at a density of $3x10^5$ cells/well. BM-MSCs were incubated for 18-24 h and transfected using a Lipofectamine 2000 kit (Sigma-Aldrich; Merck KGaA). Liposomes, si-NC, si- X-inactive specific transcript (XIST), pcDNA-NC and pcDNA-XIST were all purchased from Shanghai Genechem (Shanghai, China). Detailed cell transfection was performed according to the instructions. siRNA at the concentration of 50 nM was added to each well and then incubated for 48 h. The sequences of the three si-XISTs were as follows: si-XIST 1#, 5'-GGCCTG TTATGTGTGTGATTATATT-3'; si-XIST 2#, 5'-GCCAAC TGTCTGCTTAAGAAA-3'; and si-XIST 3#, 5'-GCTGCT AGTTTCCCAATGATA-3'.

*Alkaline phosphatase (ALP) staining*. ALP staining was performed using the ALP detection kit (Sigma Aldrich; Merck KGaA) according to the manufacturer's instructions. MSCs were seeded in 24-well plates at a density of 7x10 4 cells/well. Differentiation into osteoblasts was induced by osteogenic induction medium at a cell density of 60%. Following 10 days of induction, the cells were fixed with 4% formaldehyde and 5% citrate in acetone at room temperature for 30 sec. The fixed cells were further washed with PBS and incubated with 0.2% naphthol AS-BI and 0.2% diazonium salt for 15 min at room temperature. Once the working solution was discarded, the cells were washed with PBS again. Images were captured using a light microscope at a magnification of x4.

*Alizarin Red S (ARS) staining*. The morphology of BM-BMSCs was observed with a microscope. Once the medium was discarded, the cells were washed twice with PBS and then fixed with 1 ml 4% paraformaldehyde at 20˚C for 20 min. Cells were then washed twice with PBS. Following this, cells were stained with 1 ml ARS at room temperature for 10 min. The cell samples were washed twice with PBS for 10 min each and images were captured with an optical microscope (magnification, x4).

*Statistical analysis*. Statistical analyses were performed with SPSS software (v22.0; IBM Corp., Armonk, NY, USA). In addition, GraphPad Prism software 5.0 (GraphPad Software, Inc., La Jolla, CA, USA) was used for image editing. Comparisons between multiple groups were performed using one-way analysis of variance followed by a post hoc test (Fisher's Least Significant Difference). $P<0.05$ was considered to indicate a statistically significant difference.

## Results

*Alterations in the expression levels of 6 lncRNAs in patients with OP*. Data were merged using the combat method and the Slicomerging R package, and the differentially expressed genes were calculated in accordance with the RankProd method. The results indicated that there were 1,060 downregulated genes and 765 upregulated genes, in which there were 4 upregulated lncRNAs and 2 downregulated lncRNAs (Fig. 1A and Table I), including LOC100507630, IGHV4-31, GRIK1-AS2, DKFZP586I1420, THAP9-AS1 and XIST. XIST is an important lncRNA that has been previously reported in a variety of diseases, but not in OP (25,26).

Table I. Significantly dysregulated probes identified by RankProd in osteoporosis.

| ID | Symbol | FC_class1.class2 | pfp | P-value |
|---|---|---|---|---|
| 207476_at | LOC100507630 | 0.886603422 | 0 | <0.001 |
| 217281_x_at | IGHV4-31 | 0.823655383 | $1.00x10^{-04}$ | <0.001 |
| 210818_s_at | GRIK1-AS2 | 1.091941472 | 0 | <0.001 |
| 213546_at | DKFZP586I1420 | 1.107174491 | $2.00x10^{-04}$ | <0.001 |
| 215009_s_at | THAP9-AS1 | 1.153535587 | $4.00x10^{-04}$ | <0.001 |
| 221728_x_at | XIST | 1.045369015 | 0.0029 | $1.00x10^{-04}$ |

pfp<0.01; FC>1. pfp, proportion of false positives; FC, fold change.

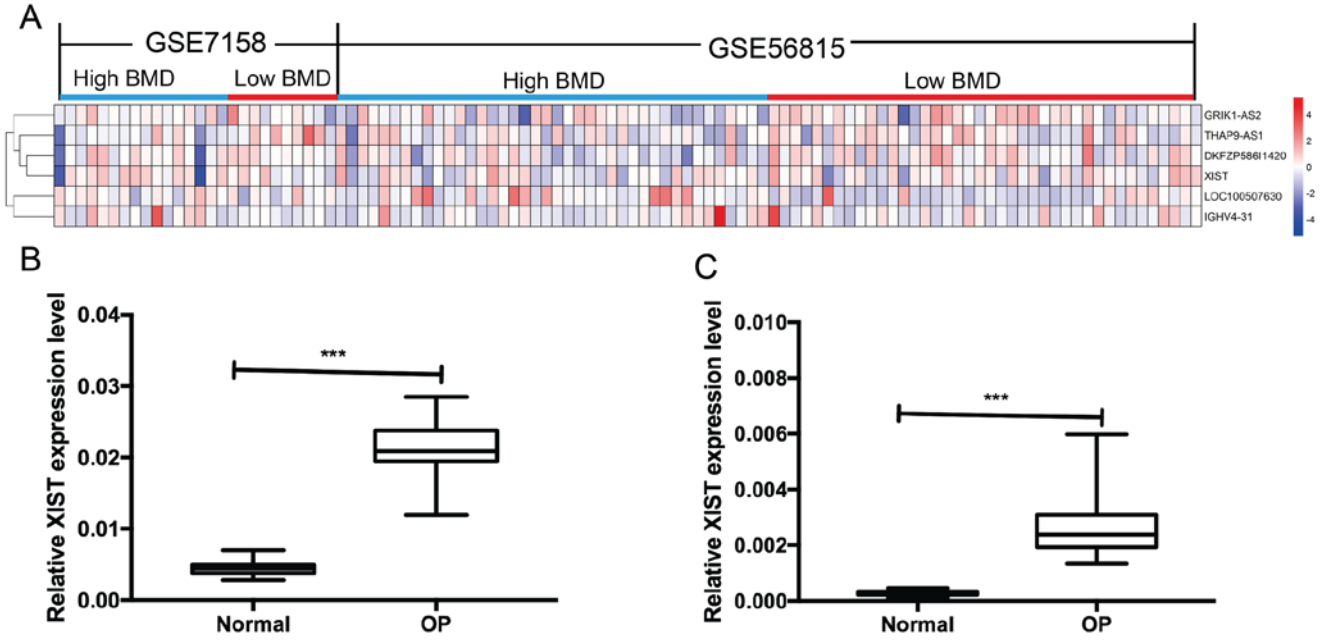


Figure 1. Dysfunctional expression of lncRNA in monocytes of patients with OP. (A) Six lncRNAs is dysregulated in OP in monocyte. (B) XIST is upregulated in monocytes from patients with OP. (C) XIST is upregulated in serum from patients with OP. ***P<0.001. LncRNA, long non-coding RNa; OP, osteoporosis; XIST, X-inactive specific transcript.

Therefore, XIST was chosen as a candidate lncRNA to explore its associated mechanism in OP. The expression of lncRNA XIST in serum and peripheral blood monocytes was detected by RT-qPCR in patients with OP and normal subjects. The results indicated that the expression level of lncRNA XIST in the serum and peripheral blood monocytes of patients with OP was significantly increased compared with that in normal subjects (Fig. 1B and C).

*BM-MSCs purity*. Primary BM-MSCs were isolated from rat bone marrow and passaged successfully. BM-MSCs adhered to plastic cultured dishes and exhibited a typical spindle-shaped morphology (Fig. 2A). Following 14 days of osteogenic induction, a large number of mineralized nodules were observed, as demonstrated by ARS staining (Fig. 2B). The immunophenotype was identified by flow cytometry. As demonstrated in Fig. 2C, the results indicated that the isolated cells were positive for mesenchymal-associated markers CD29 (99.82%), CD44 (99.73%) and CD90 (99.68%). However, few cells were positive for CD45 (0.01%). A large number of calcified nodules were identified by ARS staining following 14 days of culture in osteogenic medium. However, this was not observed in the control group, which demonstrated the ability of the MSCs to differentiate into osteoblasts. In order to further verify that BM-MSCs could be differentiated into osteoblasts, the osteogenic marker genes ALP, runt related transcription factor 2 (Runx2) and bone γ-carboxyglutamic acid-containing protein (Bglap) were detected in cells cultured for 1, 3, 7 and 14 days. On the 3rd and 7th day, the expression levels of the marker genes mentioned above were significantly increased (Fig. 2D). By contrast, the expression level of XIST in the cells was significantly decreased in a time-dependent manner (Fig. 2E).

*XIST inhibits osteogenic differentiation of BM-MSCs*. To investigate the effect of XIST on the expression of the osteogenic marker genes, RT-qPCR was performed (Fig. 3). Following si-XIST transfection, the expression level of

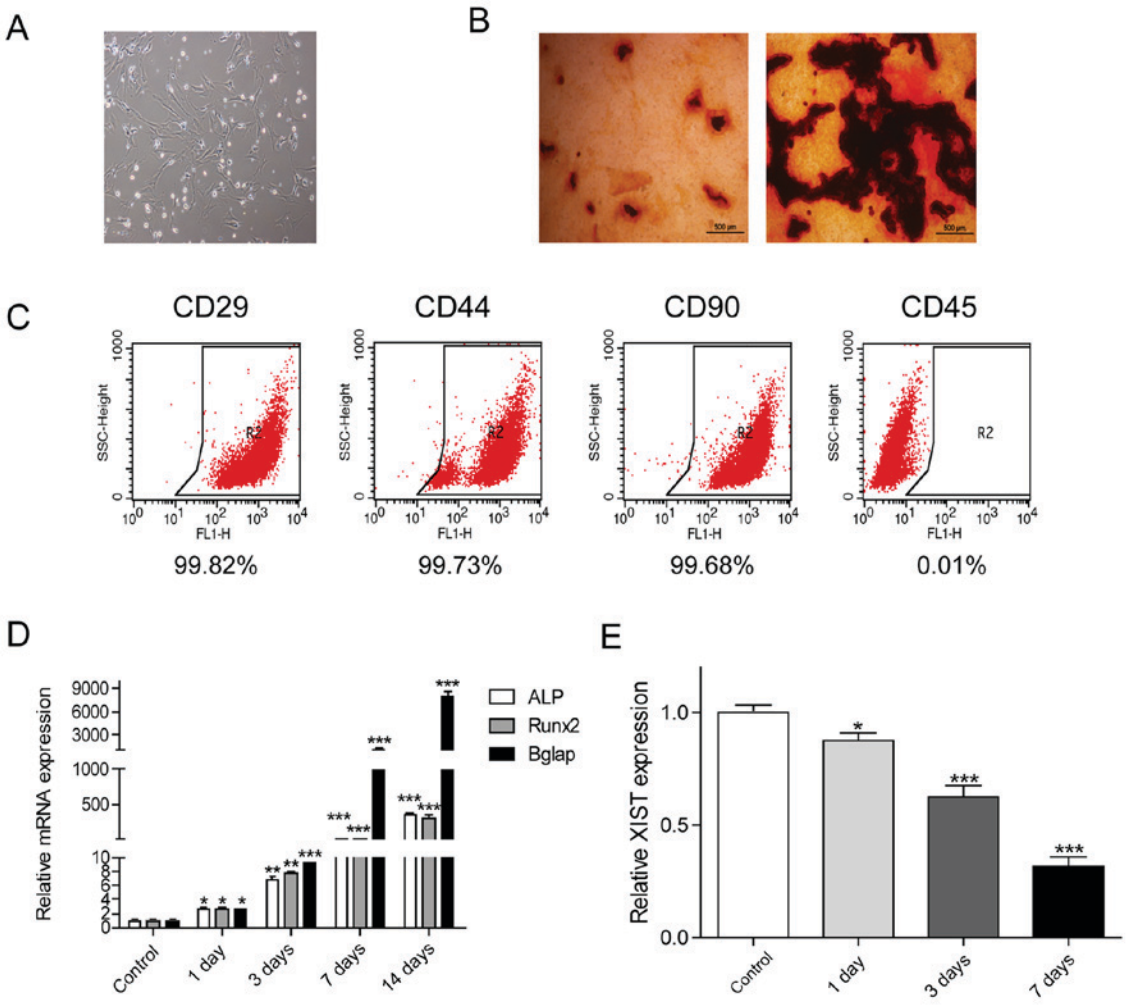


Figure 2. Phenotypic identification of bone marrow mesenchymal stem cells. (A) The shape of MSCs on the 4th day. A typical long fusiform shape was observed in the MSCs (magnification, x40). (B) Following cultured in osteogenic induction medium for 14 days, MSCs exhibited more mineralized nodules according to Alizarin Red S staining, whereas the control group did not. (C) Identification of MSC-specific surface antigens, including positive identification of CD29, CD44 and CD90, and negative identification of CD45 using flow cytometry. (D) The expression levels of osteoblast marker genes ALP, Runx2 and Bglap on different days of induction were significantly increased most obviously on the 3rd and 7th day of induction. (E) The expression of XIST decreased in a time-dependent manner. $^{*}$P<0.05, $^{**}$P<0.01 and $^{***}$P<0.001 vs. the control group. MSCs, mesenchymal stem cells; XIST, X-inactive specific transcript; ALP, alkaline phosphatase; Runx2, runt related transcription factor 2; Bglap, bone γ-carboxyglutamic acid-containing protein; CD, cluster of differentiation.

XIST in BM-MSCs was significantly reduced, and the most significant decrease was induced by si-XIST 2# (Fig. 3A). Subsequently, si-XIST2 was selected for the remaining interference experiments. Notably, XIST expression levels were significantly increased with pcDNA-XIST transfected in BM-MSCs, which confirmed the transfection efficiency (Fig. 3B).

The expression levels of ALP, Bglap and Runx2 genes were significantly increased by si-XIST 2# (Fig. 3C, E and G). Conversely, the expression levels of the above osteoblast-associated genes were significantly reduced following the overexpression of XIST (Fig. 3D, F and H). Correspondingly, the expression trends of ALP and Runx2 proteins were consistent with their relative RNAs (Fig. 4A). Furthermore, ALP staining was enhanced following XIST interference and reduced with XIST overexpression (Fig. 4B).

Following interfering with XIST, the number of mineralized nodules was increased, as indicated with the increased ARS staining. Conversely, smaller and fewer nodules were observed when XIST was overexpressed (Fig. 4C). These results suggested that overexpression of XIST could inhibit osteogenic differentiation of BM-MSCs.

## Discussion

In a normal cycle of bone metabolism, bone absorption and formation are in a dynamic balance. Bone absorption of osteoclasts and bone formation of osteoblasts are coupled for the continuous reconstruction of bones. However, once the coupled balance is broken, it can result in an increase in bone absorption of osteoclasts, or a decrease in bone formation of osteoblasts, thereby leading to the former process being greater than the latter, and giving rise to OP (27-29).

XIST, a lncRNA indispensable for silencing the transcription of chromosome X in mammals, is critical for the deactivation of chromosome X (25). In recent years, more studies have demonstrated that XIST is correlated with the development and progression of tumors (30-32). In

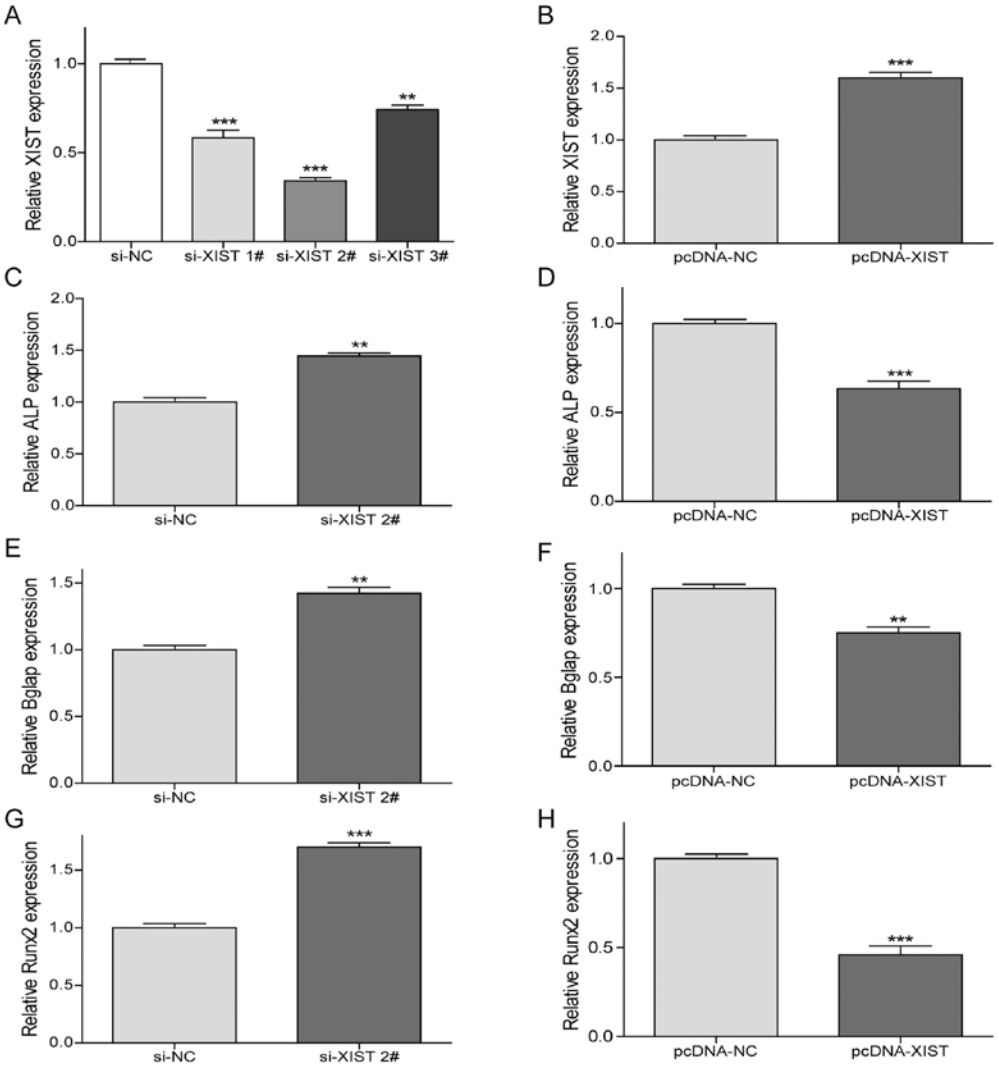


Figure 3. XIST inhibits the expression of the osteogenic marker genes. (A) Following transfection with si-XIST, the expression of XIST was indicated to be the lowest with si-XIST 2#. (B) Following overexpression of XIST, the expression of XIST in cells was significantly increased. (C and D) Expression of ALP was increased in cells following XIST inhibition but decreased in XIST-overexpressed cells. (E) Expression of Bglap was increased in cells with XIST inhibition. (F) Bglap expression was decreased in cells when the overexpression of XIST was induced. (G and H) Expression of Runx2 was increased in cells following XIST interference but decreased in XIST-overexpressed cells. $^{**}$P<0.01 and $^{***}$P<0.001 vs. the si-NC group or the pcDNA-NC group. NC, negative control; si, small interfering; XIST, X-inactive specific transcript; ALP, alkaline phosphatase; Runx2, runt related transcription factor 2; Bglap, bone γ-carboxyglutamic acid-containing protein.

glioblastoma, XIST knockdown can inhibit the progression of tumors by reducing cell proliferation, invasion and migration and inducing cell apoptosis (30). In patients with gastric cancer it has been reported that the high expression of XIST is associated with an increase in tumor volume, lymphatic metastasis, distant metastasis and tumor, node, metastasis staging (33,34). Furthermore, lncRNA maternally expressed 3 and differentiation antagonizing non-protein coding RNA are also critical for bones; however, no study has reported on the role of XIST (35,36).

Bone is a dynamic tissue that is in continuously modified (19). It is primarily composed of two types of cells, osteoblasts and osteoclasts; the former promote bone formation, while the latter promote bone resorption (19). These two types of bone cells are at equilibrium in normal bone. However, once this balance is disrupted, a variety of bone metabolic diseases can be triggered (37). Bglap and Runx2, two important markers of bone formation, are tightly bound to bone hydroxyapatite and calcium and are indirectly involved in osteoblast activation during osteogenesis (19). ALP is also an important marker of early osteogenic differentiation of BM-MSCs, which serves a key role in the *in vitro* calcification of BM-MSCs (38-40). Therefore, early osteogenic differentiation of BM-MSCs can be observed through the detection of ALP synthesis (41). Calcium nodules are formed when mineralization occurs in BM-MSCs. The formation of calcium nodules is a sign of maturation of cells (19). The degree of osteogenic differentiation of BM-MSCs can be analyzed by detecting the formation of calcium nodules in BM-MSCs (42). In the present study, RankProd analysis with the retrieval of databases demonstrated that XIST was highly expressed in patients with OP. It was indicated that overexpression of XIST significantly decreased the gene and protein expression levels of ALP, Bglap and Runx2, whereas ALP staining and calcification in ARS staining were reduced. These results indicated that XIST inhibited

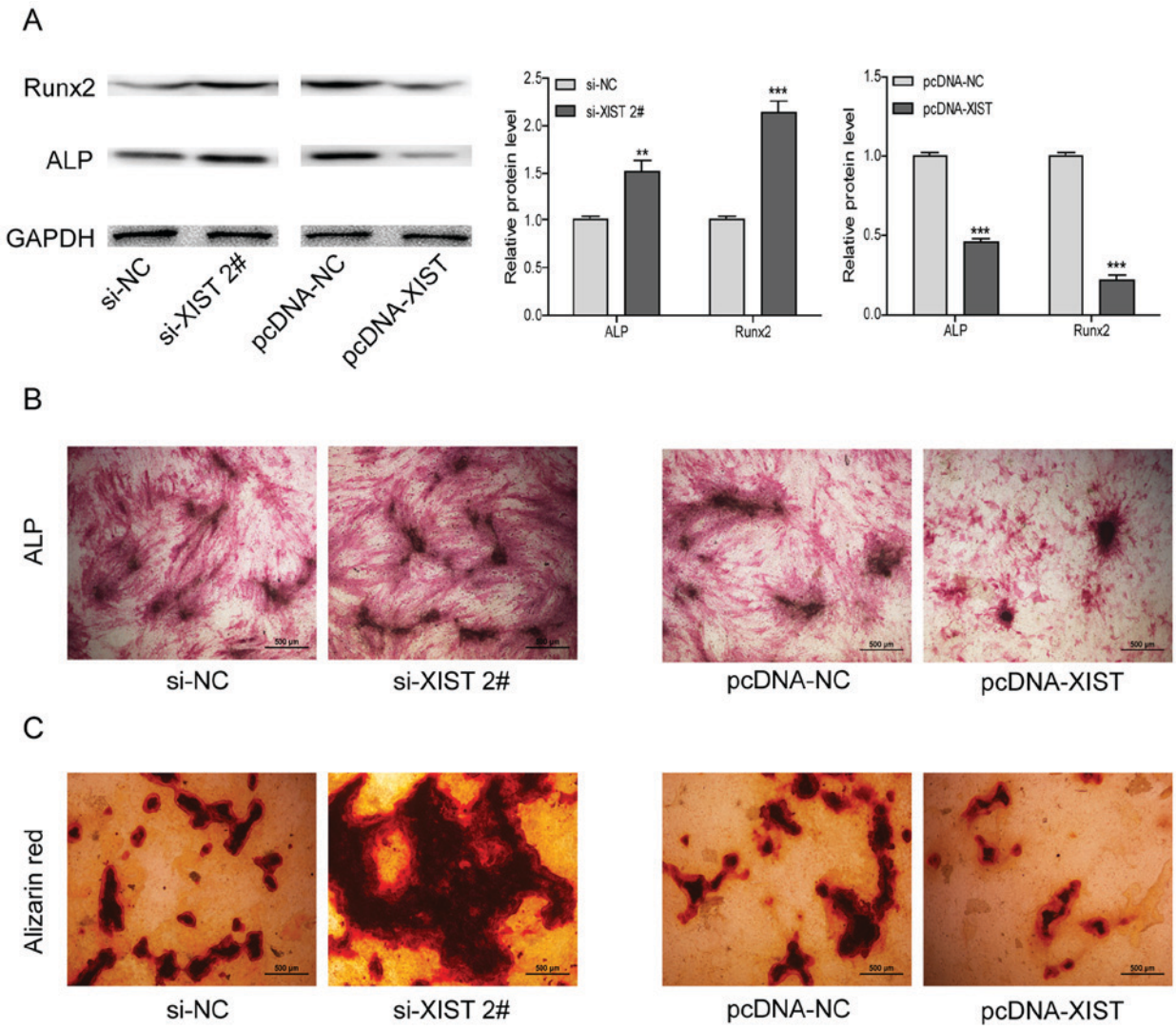


Figure 4. XIST inhibits osteogenic marker protein expression and osteogenic differentiation. (A) Expression of ALP and Runx2 protein was increased in cells following XIST inhibition but decreased in cells with overexpressed XIST. (B) Staining of ALP was increased in cells following XIST inhibition but decreased in cells with overexpressed XIST. (C) Alizarin Red S staining was increased in cells following XIST inhibition but decreased in cells with overexpressed XIST. $^{**}$P<0.01 vs. the si-NC group; $^{***}$P<0.001 vs. the si-NC group or the pcDNA-NC group. NC, negative control; si, small interfering; XIST, X-inactive specific transcript; ALP, alkaline phosphatase; Runx2, runt related transcription factor 2.

osteogenic differentiation of BM-MSCs, which was consistent with the data analysis.

The present study had some limitations. Firstly, the present study only demonstrated the association between XIST and BM-MSCs; however, the detailed molecular mechanism has not been fully elucidated. Further research should be performed to explore how XIST influences the differentiation of BM-MSCs and what types of molecules or signaling pathways takes part in this effect. Notably, si-XIST and pcDNA-XIST transgenic mice will be used in future work to investigate the development of OP, and to analyze the expression of XIST and osteoblast identification indexes.

In conclusion, the present findings suggest that XIST is highly expressed in patients with OP, and XIST is able to inhibit osteogenic differentiation of BM-MSCs.

## Acknowledgements

Not applicable.

## Funding

The current study was supported by the National Natural Science Foundation of China (grant no. 81802149) and Science and Technology Development Fund of NJMU (grant no. 2017NJMU130).

## Availability of data and materials

All data generated or analyzed during the present study are included in this published article.

## Authors' contributions

XCh, SZ and BL designed the study and performed the experiments. XCa, LY and WW established the animal models. DG, JY and ZY collected the data. XCh and CJ analyzed the data. XCh and LY prepared the manuscript. All authors read and approved the final manuscript.

## Ethics approval and consent to participate

This study was approved by the Animal Ethics Committee of Nanjing Medical University Animal Center. This study was also approved by the Medical Ethics Committee of Nanjing First Hospital (Nanjing, China) and patient consent was obtained.

## Patient consent for publication

Written informed consent was obtained from all the participants.

## Competing interests

The authors declare no competing interests.

## Refere3nces


1. Cosman F, de Beur SJ, LeBoff MS, Lewiecki EM, Tanner B, Randall S and Lindsay R: Erratum to: Clinician's guide to prevention and treatment of osteoporosis. Osteoporos Int 26: 2045-2047, 2015.
2. Ge DW, Wang WW, Chen HT, Yang L and Cao XJ: Functions of microRNAs in osteoporosis. Eur Rev Med Pharmacol Sci 21: 4784-4789, 2017.
3. Pfeilschifter J, Cooper C, Watts NB, Flahive J, Saag KG, Adachi JD, Boonen S, Chapurlat R, Compston JE, Díez-Pérez A, *et al*: Regional and age-related variations in the proportions of hip fractures and major fractures among postmenopausal women: The Global Longitudinal Study of Osteoporosis in Women. Osteoporos Int 23: 2179-2188, 2012.
4. Wang WW, Yang L, Wu J, Gao C, Zhu YX, Zhang D and Zhang HX: The function of miR-218 and miR-618 in postmenopausal osteoporosis. Eur Rev Med Pharmacol Sci 21: 5534-5541, 2017.
5. Court F, Baniol M, Hagege H, Petit JS, Lelay-Taha MN, Carbonell F, Weber M, Cathala G and Forne T: Long-range chromatin interactions at the mouse Igf2/H19 locus reveal a novel paternally expressed long non-coding RNA. Nucleic Acids Res 39: 5893-5906, 2011.
6. Garmire LX, Garmire DG, Huang W, Yao J, Glass CK and Subramaniam S: A global clustering algorithm to identify long intergenic non-coding RNA-with applications in mouse macrophages. PLoS One 6: e24051, 2011.
7. Gibb EA, Vucic EA, Enfield KS, Stewart GL, Lonergan KM, Kennett JY, Becker-Santos DD, MacAulay CE, Lam S, Brown CJ and Lam WL: Human cancer long non-coding RNA transcriptomes. PLoS One 6: e25915, 2011.
8. Korostowski L, Raval A, Breuer G and Engel N: Enhancer-driven chromatin interactions during development promote escape from silencing by a long non-coding RNA. Epigenetics Chromatin 4: 21, 2011.
9. Muers M: RNA: Genome-wide views of long non-coding RNAs. Nat Rev Genet 12: 742, 2011.
10. Saxena A and Carninci P: Long non-coding RNA modifies chromatin: Epigenetic silencing by long non-coding RNAs. Bioessays 33: 830-839, 2011.
11. Schorderet P and Duboule D: Structural and functional differences in the long non-coding RNA hotair in mouse and human. PLoS Genet 7: e1002071, 2011.
12. Yang Z, Zhou L, Wu LM, Lai MC, Xie HY, Zhang F and Zheng SS: Overexpression of long non-coding RNA HOTAIR predicts tumor recurrence in hepatocellular carcinoma patients following liver transplantation. Ann Surg Oncol 18: 1243-1250, 2011.
13. Lorenzen JM, Schauerte C, Kielstein JT, Hubner A, Martino F, Fiedler J, Gupta SK, Faulhaber-Walter R, Kumarswamy R, Hafer C, *et al*: Circulating long noncoding RNATapSaki is a predictor of mortality in critically ill patients with acute kidney injury. Clin Chem 61: 191-201, 2015.
14. Kumarswamy R, Bauters C, Volkmann I, Maury F, Fetisch J, Holzmann A, Lemesle G, de Groote P, Pinet F and Thum T: Circulating long noncoding RNA, LIPCAR, predicts survival in patients with heart failure. Circ Res 114: 1569-1575, 2014.
15. Yang KC, Yamada KA, Patel AY, Topkara VK, George I, Cheema FH, Ewald GA, Mann DL and Nerbonne JM: Deep RNA sequencing reveals dynamic regulation of myocardial noncoding RNAs in failing human heart and remodeling with mechanical circulatory support. Circulation 129: 1009-1021, 2014.
16. Orsmark-Pietras C, James A, Konradsen JR, Nordlund B, Söderhäll C, Pulkkinen V, Pedroletti C, Daham K, Kupczyk M, Dahlen B, *et al*: Transcriptome analysis reveals upregulation of bitter taste receptors in severe asthmatics. Eur Respir J 42: 65-78, 2013.
17. Liu Z, Li X, Sun N, Xu Y, Meng Y, Yang C, Wang Y and Zhang K: Microarray profiling and co-expression network analysis of circulating lncRNAs and mRNAs associated with major depressive disorder. PLoS One 9: e93388, 2014.
18. Peng H, Liu Y, Tian J, Ma J, Tang X, Rui K, Tian X, Mao C, Lu L, Xu H, *et al*: The long noncoding RNA IFNG-AS1 promotes T helper type 1 cells response in patients with hashimoto's thyroiditis. Sci Rep 5: 17702, 2015.
19. Mundy GR and Elefteriou F: Boning up on ephrin signaling. Cell 126: 441-443, 2006.
20. Tang Y, Wu X, Lei W, Pang L, Wan C, Shi Z, Zhao L, Nagy TR, Peng X, Hu J, *et al*: TGF-beta1-induced migration of bone mesenchymal stem cells couples bone resorption with formation. Nat Med 15: 757-765, 2009.
21. Soen S, Fukunaga M, Sugimoto T, Sone T, Fujiwara S, Endo N, Gorai I, Shiraki M, Hagino H, Hosoi T, *et al*: Diagnostic criteria for primary osteoporosis: Year 2012 revision: J Bone Miner Metab 31: 247-257, 2013.
22. Breitling R, Armengaud P, Amtmann A and Herzyk P: Rank products: A simple, yet powerful, new method to detect differentially regulated genes in replicated microarray experiments. FEBS Lett 573: 83-92, 2004.
23. Taminau J, Meganck S, Lazar C, Steenhoff D, Coletta A, Molter C, Duque R, de Schaetzen V, Weiss Solís DY, Bersini H and Nowé A: Unlocking the potential of publicly available microarray data using inSilicoDb and inSilicoMerging R/Bioconductor packages. BMC Bioinformatics 13: 335, 2012.
24. Livak KJ and Schmittgen TD: Analysis of relative gene expression data using real-time quantitative PCR and the 2(-Delta Delta C(T)) method. Methods 25: 402-408, 2001.
25. Yue M, Ogawa A, Yamada N, Charles Richard JL, Barski A and Ogawa Y: Xist RNA repeat E is essential for ASH2L recruitment to the inactive X and regulates histone modifications and escape gene expression. PLoS Genet 13: e1006890, 2017.
26. Li GL, Wu YX, Li YM and Li J: High expression of long non-coding RNA XIST in osteosarcoma is associated with cell proliferation and poor prognosis. Eur Rev Med Pharmacol Sci 21: 2829-2834, 2017.
27. Cheung AM, Papaioannou A and Morin S; Osteoporosis Canada Scientific Advisory Council: Postmenopausal osteoporosis. N Engl J Med 374: 2096, 2016.
28. Tsai JN, Uihlein AV, Lee H, Kumbhani R, Siwila-Sackman E, McKay EA, Burnett-Bowie SA, Neer RM and Leder BZ: Teriparatide and denosumab, alone or combined, in women with postmenopausal osteoporosis: The DATA study randomised trial. Lancet 382: 50-56, 2013.
29. Rachner TD, Khosla S and Hofbauer LC: Osteoporosis: Now and the future. Lancet 377: 1276-1287, 2011.
30. Yao Y, Ma J, Xue Y, Wang P, Li Z, Liu J, Chen L, Xi Z, Teng H, Wang Z, *et al*: Knockdown of long non-coding RNA XIST exerts tumor-suppressive functions in human glioblastoma stem cells by up-regulating miR-152. Cancer Lett 359: 75-86, 2015.
31. Tantai J, Hu D, Yang Y and Geng J: Combined identification of long non-coding RNA XIST and HIF1A-AS1 in serum as an effective screening for non-small cell lung cancer. Int J Clin Exp Pathol 8: 7887-7895, 2015.
32. Sirchia SM, Tabano S, Monti L, Recalcati MP, Gariboldi M, Grati FR, Porta G, Finelli P, Radice P and Miozzo M: Misbehaviour of XIST RNA in breast cancer cells. PLoS One 4: e5559, 2009.
33. Ma L, Zhou Y, Luo X, Gao H, Deng X and Jiang Y: Long non-coding RNA XIST promotes cell growth and invasion through regulating miR-497/MACC1 axis in gastric cancer. Oncotarget 8: 4125-4135, 2017.
34. Chen DL, Ju HQ, Lu YX, Chen LZ, Zeng ZL, Zhang DS, Luo HY, Wang F, Qiu MZ, Wang DS, *et al*: Long non-coding RNA XIST regulates gastric cancer progression by acting as a molecular sponge of miR-101 to modulate EZH2 expression. J Exp Clin Cancer Res 35: 142, 2016.

35. Tong X, Gu PC, Xu SZ and Lin XJ: Long non-coding RNA-DANCR in human circulating monocytes: A potential biomarker associated with postmenopausal osteoporosis. Biosci Biotechnol Biochem 79: 732-737, 2015.
36. Wang Q, Li Y, Zhang Y, Ma L, Lin L, Meng J, Jiang L, Wang L, Zhou P and Zhang Y: LncRNA MEG3 inhibited osteogenic differentiation of bone marrow mesenchymal stem cells from postmenopausal osteoporosis by targeting miR-133a-3p. Biomed Pharmacother 89: 1178-1186, 2017.
37. Pagani F, Francucci CM and Moro L: Markers of bone turnover: Biochemical and clinical perspectives. J Endocrinol Invest 28 (10 Suppl): S8-S13, 2005.
38. Johansen JS, Riis BJ, Delmas PD and Christiansen C: Plasma BGP: An indicator of spontaneous bone loss and of the effect of oestrogen treatment in postmenopausal women. Eur J Clin Invest 18: 191-195, 1988.
39. Enomoto H, Furuichi T, Zanma A, Yamana K, Yoshida C, Sumitani S, Yamamoto H, Enomoto-Iwamoto M, Iwamoto M and Komori T: Runx2 deficiency in chondrocytes causes adipogenic changes in vitro. J Cell Sci 117: 417-425, 2004.
40. Bai Y, Yin G, Huang Z, Liao X, Chen X, Yao Y and Pu X: Localized delivery of growth factors for angiogenesis and bone formation in tissue engineering. Int Immunopharmacol 16: 214-223, 2013.
41. Golub EE, Harrison G, Taylor AG, Camper S and Shapiro IM: The role of alkaline phosphatase in cartilage mineralization. Bone Miner 17: 273-278, 1992.
42. Giannoudis PV, Jones E and Einhorn TA: Fracture healing and bone repair. Injury 42: 549-550, 2011.vv